ISSN 1330-3651 (Print), ISSN 1848-6339 (Online)
https://doi.org/10.17559/TV-20230311001094
Original scientific paper

Structural Integrity Assessment of Spherical Tanks for Propane Butane Gas Storage

Hana R. QANANAH, Radovan PETROVIĆ*, Maja ANDJELKOVIĆ, Boris DAMJANOVIĆ, Igor MARTIĆ, Ivana VUČETIĆ, Gordana DJUKANOVIĆ

Abstract: Structural integrity analysis of spherical tank is presented based on use of experimental results, together with the analytical and numerical ones. Analytical calculation of stresses in the scope of design process is shortly presented. Numerical analysis was performed by using the Finite Element Method (FEM) to identify areas with high stress concentration, indicating that stress values near supports reach the yield stress. FEM results were verified by the experiment, indicating that it was not necessary to reinforce the spherical tank supports, since its integrity was not jeopardized in normal working conditions. This was also proved by repeating the experiment after 8 months of exploitation.

Keywords: analytical calculation; finite element method; spherical tanks; strain gauges; structural integrity

1 INTRODUCTION

Structural integrity is relatively new scientific discipline, based on fracture mechanics principles, which goes beyond common design rules to take into account cracks and other unacceptable defects, as shown in different aspects in [1-8]. Yet another step into more safe operation of critical components, like pressure vessels, was the introduction of risk based analysis, in combination with fracture mechanics and structural integrity assessment, [9-11]. Among them, paper [9] is of special interest, since the novel procedure of pressure vessels integrity assessment was introduced and explained. In any case, these analyses are based on the stress state calculations, as done by analytical and finite element method (FEM) [12-14].

In this paper the spherical tank for propane-butane gas (Fig. 1) was analysed, using a combination of analytical and FEM calculation, as well as experimental testing, to define stress and strain state as precise as possible as presented also in [15-18].

Figure 1 Spherical tank

One important aim of this analysis is to indicate areas where the equivalent stress reaches and/or exceeds the yield stress, and what would be the consequences, as also shown in [15-22]. Toward this aim, FEM is the most efficient and reliable engineering tool, but one should keep in mind that its accuracy depends on mesh quality, proper constraints, as well as loads and boundary conditions, [17-19]. Therefore, experimental verification of FEM results is of utmost interest, especially in the critical areas, [20]. Combination of analytical procedure with FEM analysis and experimental testing of spherical tank gives a more detailed insight into the behaviour of tank construction in most critical areas in comparison to a design process which relies solely on analytical results thus ensuring optimum design and safe usage during envisioned working life time. Basic data for the analysis was:

- Outer Radius 5260 mm
- Thickness 24 mm
- Material high strength low alloy steel NIOVAL 47 (yield strength 470 MPa, tensile strength 590 MPa)
- Working pressure 1.67 MPa.

2 ANALYTICAL CALCULATIONS

Analytical calculation of the spherical tank stress state, represented as the thin shell under membrane load, Fig. 2, is presented in details in [23-26]. Here, only basic equilibrium equations are presented in the following form:

$$\frac{\partial N_\theta}{\partial \theta} r_1 + N_{\theta\varphi} r_1 \cos\varphi + \frac{\partial \left(N_{\varphi\theta} r_0 \right)}{\partial \varphi} + X r_0 r_1 = 0 \tag{1a}$$

$$\frac{\partial N_{\theta\varphi}}{\partial \theta} r_1 - N_\theta r_1 \cos\varphi + \frac{\partial \left(N_\varphi r_0 \right)}{\partial \varphi} + X r_0 r_1 = 0 \tag{1b}$$

$$\frac{N_\theta}{r_2} + \frac{N_\varphi}{r_1} = -Z \tag{1c}$$

By solving Eqs. (1a-c) one can get solutions for displacements, strains and stresses, as presented in more details in [23-26].

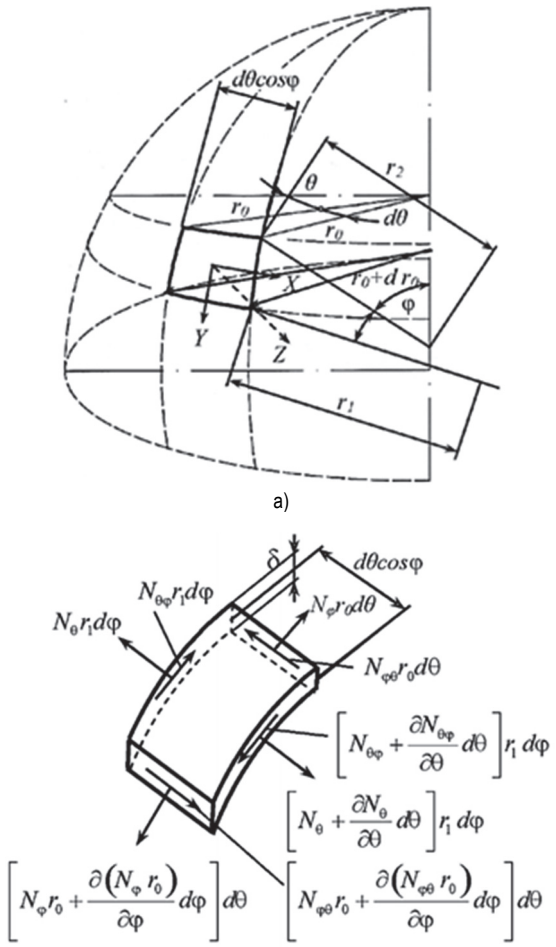

Figure 2 a) Position of the shell in the form of surface of revolution; b) Internal forces in the element of the shell, [26]

3 FINITE ELEMENT METHOD

Fig. 3 shows the finite element mesh and basic data of the storage tank, supported on 8 symmetrically placed legs, analyzed for two cases.

In the first case, the tank is supported on 8 supports symmetrically placed, so that only one-eighth of the tank can be analyzed. An angle $\alpha = 90°$ is adopted here, and fixed points of support are indicated by reinforced lines (between nodes 38 and 47, etc.). An overpressure of $p_g =$ 16.7 bar, hydrostatic pressure-height of liquid $H_1 = R$ and own weight were taken into account in both cases.

In the second case, the support is performed along a circular line (nodes 38, 46).

Working internal pressure was $p_g = 16.7$ bar, whereas hydrostatic pressure due to fluid with height $H_1 = R$ and storage tank own weight were taken into account additionally. Typical results for displacements are shown in Fig. 4, i.e. radius enlargement, including hydrostatic pressure effects, such as an increase from 8.85 mm to 9.76 mm. Uneven distribution of displacement can be explained by the effect of the supports.

Fig. 5 presents distribution of the first principal stress σ_1 for the vertical plane. One can see that the principal stress σ_1 increased in the case of line support due to constraint along the line 38-46.

The uniform distribution of the principal stress is due to the membrane state of the stress and that only constraint along the line 38-46 makes some difference.

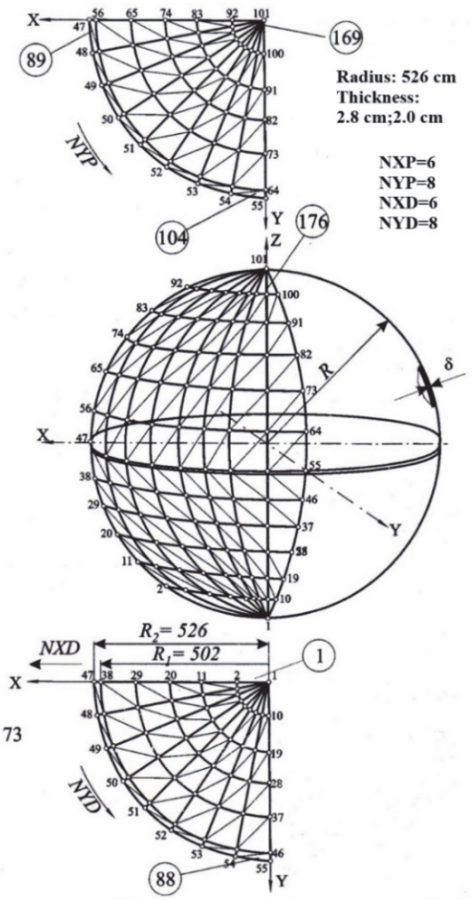

Figure 3 Finite element mesh

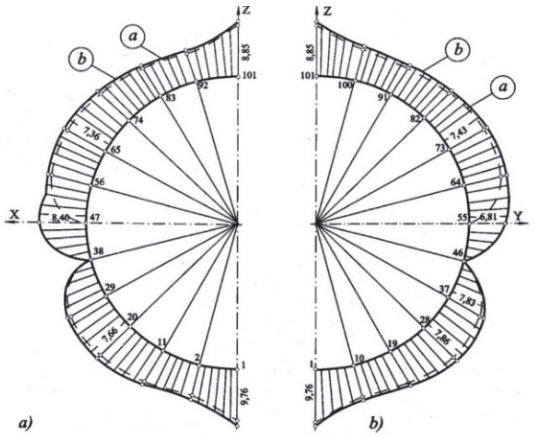

Figure 4 Displacement distribution in radial direction

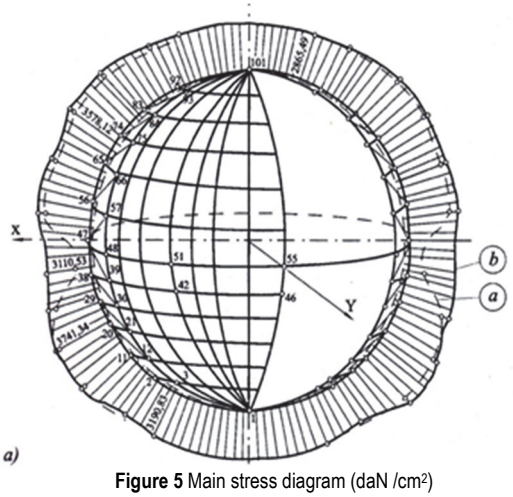

Figure 5 Main stress diagram (daN /cm²)

4 EXPERIMENTAL VERIFICATION

Analytical and FEM results are verified by experimental testing performed with water pressurizing. The experiment was carried out by measuring stresses at 7 measuring points with 21 strain gauges, by using the measuring equipment HBM UPM 100, as shown in Fig. 6. This type of strain gauges setup makes measuring easier and does not require knowledge of the direction of the principal stresses. The strain gauges placed near supports are shown in Fig. 7.

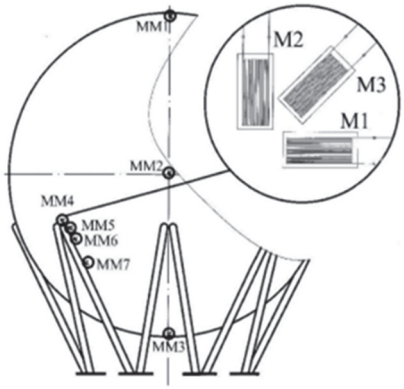

Figure 6 The layout of the measuring points, [26]

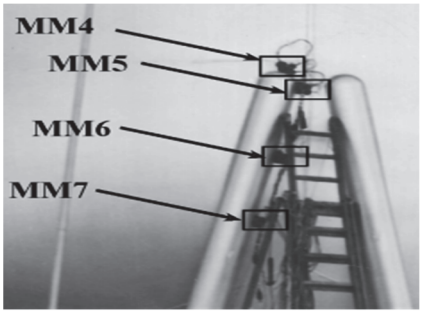

Figure 7 Strain gauges MM4÷MM7, [26]

Stress values for the working pressure of 1.67 MPa, obtained analytically, by FEM and experimentally, are presented in Tab. 1.

Table 1 Analytical, numerical and experimental stresses (working pressure), [26]

Measuring site	σ_e / MPa Analytical	σ_e / MPa FEM	σ_e / MPa Experimental
MM 1	185.3	183.5	169.6
MM 2	192.4	190.1	175.6
MM 3	199.1	197.0	182.3
MM 4	-	334.8	343.1
MM 5	194.6	199.5	201.0
MM 6	195.7	194.3	180.1
MM 7	196.6	195.4	182.3

Tab. 2 presents differences in analytical and numerical equivalent stresses, as compared with experimental ones.

Table 2 Percent difference of equivalent stresses (working pressure), [26]

Measuring site	Difference analytically / %	Difference FEM / %
MM 1	9.3	8.2
MM 2	9.6	8.3
MM 3	9.2	8.1
MM 4	-	2.4
MM 5	3.2	0.7
MM 6	8.7	7.9
MM 7	7.8	7.2

The equivalent stresses obtained by the test pressure of 2.5 MPa are shown in Tab. 3, whereas the differences of analytical and numerical results, as compared to experimental ones are shown in Tab. 4. One should notice the experimental values are typically lower than the analytical ones, up to 12.6%, as well as compared with the numerical ones, but only up to 6.7%, if MM4 is excluded. This measuring point requires special attention, since the equivalent stress is significantly higher than elsewhere. In this case experimental value is 8.1% higher than numerical one. Analytical value is missing due to the limits of procedure applied, so that stress concentration cannot be handled. It is also clear that the numerical results are not precise enough since the mesh was not refined accordingly in the area of high stress concentration.

Table 3 Analytical, numerical and experimental stresses (test pressure), [26]

Measuring site	σ_e / MPa Analytical	σ_e / MPa FEM	σ_e / MPa Experimental
MM 1	277.4	274.1	256.9
MM 2	284.4	250.3	262.9
MM 3	291.2	288.5	272.9
MM 4	-	444.1	483.4
MM 5	287.8	265.5	282.3
MM 6	289.6	257.9	257.3
MM 7	290.8	259.6	261.6

Table 4 Percent difference of equivalent stresses (working pressure), [26]

Measuring site	Deviation analytically / %	Deviation FEM / %
MM 1	8.0	6.7
MM 2	8.2	4.8
MM 3	6.7	5.7
MM 4	-	8.1
MM 5	1.9	6.0
MM 6	12.6	0.2
MM 7	11.2	0.8

From Tab. 2 and Tab. 4 one can see that numerical results match experimental ones much better than analytical results. Also, one should notice that the equivalent stress at measuring point MM4 is close to the yield stress. Having this in mind, one can also explain slight deviation from proportionality of stress values in Tabs. 1 and 3. Anyhow, plastic strain, if any, is localized, and no deformation was visible after removing the load.

5 STRUCTURAL INTEGRITY ANALYSIS

Structural integrity analysis is based on linear elastic fracture mechanics parameter, the stress intensity factor, K_I, representing load and structural geometry, including crack, while its critical value, K_{Ic}, is a material property. Using this interpretation, one can establish simple criteria for structural integrity:

$K_I \leq K_{Ic}$ - structure is safe from brittle fracture, (2a)

$K_I > K_{Ic}$ - brittle fracture is possible. (2b)

On the other side, constructions made of ductile steels, including welded joints, although less susceptible to brittle fracture, are sensitive to the plastic collapse. Therefore, more general, two-parameter approach, is used here, based on the Failure Analysis Diagram (FAD), including the limit curve, [9]:

$$K_r = S_r\left[\frac{8}{\pi^2}\ln\sec\left(\frac{\pi}{2}S_r\right)\right]^{-\frac{1}{2}} \quad (3)$$

where $K_r = K_I/K_{Ic}$, $K_I = \sigma\sqrt{\pi a}$, σ is remote stress, a crack length, K_{Ic} fracture toughness, $S_r = \sigma_{net}/\sigma_c$, σ_{net} net stress in cracked cross-section and σ_c yield criterion, commonly taken as half the value of yield and tensile strength. Reasoning behind this approach is that a completely ductile material will fail due to plastic collapse at $S_r = 1$, while a completely brittle material will fracture at $K_r = 1$. Anyhow, most of materials would fail in between these two extremes if the working point (K_r, S_r) is above the limit curve, defined by the Eq. (3), Fig. 8. On the other side, a structure is safe, if the working point is below the limit line, Fig. 8. One should notice that if a point is close to 0, the likelihood of failure is also close to 0, while for a point close to limit line the likelihood is close to 1, as introduced and explained in [9].

The FAD is now used to assess structural integrity of the storage tank presented here. The fracture toughness K_{Ic} for the weld metal is taken as 1580 MPa$\sqrt{}$mm, [9]. For the case of a crack-like defect with length $a = 1$ mm (actually depth, for a long crack along any of the weldments), the stress intensity factor can be calculated as follows:

$$K_I = Y(a/W)\sigma\sqrt{\pi a}$$

where $Y(a/W) \approx 1$ in the case of short crack, i.e. small values of a/W (0.035 for $a = 1$ mm, $W = 24$ mm - thickness), $\sigma = 343.1$ MPa (Tab. 1), $R = 5260$ mm, resulting in the ratio $K_I/K_{Ic} = 608.1/1580 = 0.38$.

Ratio between critical cross-section stress and critical stress (half of the sum of yield stress, 470 MPa, and tensile strength, 590 MPa) is calculated as follows:

$$S_R = \sigma_{net}/\sigma_c = 357.4/530 = 0.68.$$

The coordinates of the point in the FAD (0.68; 0.38) are in the safe area, Fig. 8, at the level of fracture probability approximately 0.68.

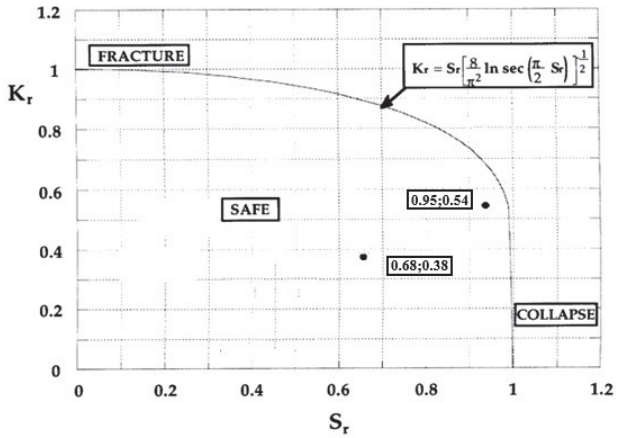

Figure 8 Failure analysis diagram

In the case of testing pressure (corresponding stress σ = 483.4 MPa) the coordinates are (0.95; 0.54) which is very close to the limit line, with fracture probability of 96%. Therefore, the critical pressure would be just 4% higher, i.e. 2.6 MPa (corresponding stress 503.5 MPa). This is yet another example of how damaging water over-pressure can be and how unnecessary it is, as explained also in [11]. Simple fact is that the only effect of over-pressure is possible damage and crack initiation in otherwise sound material that can cause failure later on. This is especially problem for welded joints. One should keep in mind that welded joints are already tested by NDT, 100% in case of "critical" pressure vessels, making over-pressure completely useless!

Finally, the application of risk-based assessment of cracked pressure vessels can be performed by applying the risk matrix to estimate risk level according to the likelihood and consequence of failure, as shown in [9]. Brief description of consequence categories is given elsewhere, [10], while here we just state that consequences are high.

Table 5 Risk levels in relation to consequences and probability in risk matrix, [12]

		Consequence category					
		1 very low	2 low	3 med.	4 high	5 very high	Risk level
Probability category	≤ 0.2 very low						Very low
	0.2-0.4 low						Low
	0.4-0.6 medium						Medium
	0.6-0.8 high				**work load**		High
	0.8-1.0 very high				**test load**		Very high

One can see that assumed crack of 1 mm in depth is a bit of a problem from the structural integrity point of view, since it produces high level of risk, but is still on the safe side. Contrary to that, testing load is a big problem since its point in FAD is very close to the limit line and risk is very high. One should also notice that even a slighty longer crack would make the test load a dangereous event.

6 CONCLUSIONS

Based on the results presented here, one can conclude the following:

- Analytical methods cannot provide precise results in the areas of stress concentration. Contrary to that numerical results are very close to experimental ones.
- From the structural integrity point of view spherical tank analysed here is safe enough even with 1 mm deep crack, but only under working load. If the test load is performed made with over-pressure 50%, very high risk is the consequence, with likelihood close to 1.

Acknowledgements

This research is supported by the Ministry of Education, Science and Technological Development, Republic of Serbia, Grant TR32036 and Contract No. 451-03-47/2023-01/200213.

7 REFERENCES

[1] Sedmak, A., Kovic, M., &Kirin, S. (2022). Structural Integrity - historical context. *Technical Gazette*, *29*(5), 1770-1776. https://doi.org/10.17559/TV-20220321074430

[2] Jeremić, L., Sedmak, A., Milovanović, N., Milošević, N., & Sedmak, S. (2021). Assessment of integrity of pressure vessels for compressed air. *Structural Integrity and Life*, *21*(1), 3-6.

[3] Sedmak, A., Arsić, M., Šarkoćević, Ž., Medjo, B., Rakin, M., Arsić, D., & Lazić, V. (2020). Remaining strength of API J55 steel casing pipes damaged by corrosion. *International Journal of Pressure Vessels and Piping*, *188*, 104230. https://doi.org/10.1016/j.ijpvp.2020.104230
[4] Gubeljak, N., Chapetti, M., Predan, J., & Landes, J. D. (2011). CTOD-R curve construction from surface displacement measurements. *Engineering Fracture Mechanics*, *78*(11), 2286-2297. https://doi.org/10.1016/j.engfracmech.2011.05.002
[5] Katinić, M., Kozak, D., Božić, Ž., & Gelo, I. (2019). Plastic limit pressures for cracked tube containing twin collinear axial through-wall cracks. *Archive of Applied Mechanics, 89*(5), 805-811. https://doi.org/10.1007/s00419-018-1395-5
[6] Kozak, D., Gubeljak, N., Konjatić, P., & Sertić, J. (2009). Yield load solutions of heterogeneous welded joints. *International Journal of Pressure Vessels and Pipings*, *86*(12), 807-812. https://doi.org/10.1016/j.ijpvp.2009.11.012
[7] Vukojević, N., Oruč, M., Vukojević, D., Hadžikadunić, & Beganović, O. (2010). Performance analysis of substitution of applied materials using fracture mechanics parameters. *Tehnički vjesnik*, *17*(4), 411-418.
[8] Gubeljak, N. (1999).The fracture behavior of specimens with a notch tip partly in the base metal of strength mis-matched welded joints. *International Journal of Fracture*, *100*(2), 169-181. https://doi.org/10.1023/A:1018777000406
[9] Golubović, T., Sedmak, A., Spasojević Brkić, V., Kirin, S., & Rakonjac, I. (2018). Novel risk based assessment of pressure vessels integrity. *Tehnički vjesnik*, *25*(3), 803-807. https://doi.org/10.17559/TV-20170829144636
[10] Vucetic, I., Kirin, S., Vucetic, T., Golubovic, T., & Sedmak, A. (2018). Risk analysis in the case of air storage tank failure at RHPP Bajina Bašta. *Structural Integrity and Life*, *18*(1), 3-6.
[11] Martić, I., Sedmak, A., Mitrović, N., Sedmak, S., & Vučetić, I. (2019). Effect of over-pressure on pipeline structural integrity. *Tehnicki vjesnik*, *26*(3), 852-855. https://doi.org/10.17559/TV-20180708213323
[12] Alnagasa, K. & Petrovic, R. (2022). Stress state analysis of propane butane gas spherical storage tanks. *Structural Integrity and Life*, *22*(2), 253-256.
[13] Milovanović, A., Martić, I., Trumbulović, L., Diković, L., & Drndarević, B. (2021). Finite element analysis of spherical storage tank stress state. *Structural Integrity and Life*, *21*(3), 273-278.
[14] Sklemina, O. Y. & Polilov, A. N. (2020). Analytical and finite element method of calculation of multi-shell gas tanks. *IOP Conference Series: Materials Science and Engineering*, *747*(1), 012131.
[15] Pramod, R., Shanmugam, N. S., Krishnadasan, C. K., & Sankaranarayanasamy, K. (2019). Finite Element Analysis of Potential Liner Failures during Operation in Spherical Pressure Vessel. *Advances in Computational Methods in Manufacturing*. https://doi.org/10.1007/978-981-32-9072-3_90
[16] Abo-Elkhier, M. &Muhammad, K. (2020). Failure analysis of an exploded large-capacity liquid storage tank using finite element analysis. *Engineering Failure Analysis*, 110, 104401. https://doi.org/10.1016/j.engfailanal.2020.104401
[17] Panthi, S. K., Ramakrishnan, N., Pathak, K. K., & Chouhan, J. S. (2007). An analysis of springback in sheet metal bending using finite element method (FEM). *Journal of Materials Processing Technology*, *186*, 120-124. https://doi.org/10. 1016/j.jmatprotec.2006.12.026
[18] Xiaodong, L., Zhongshu, H., Wenyi, D., Anfeng, Y., & Peng W. (2012). CFD Simulation of Temperature Field Distribution of the Liquefied Hydrocarbon Spherical Tank Leaking. *Procedia Engineering*, *43*, 472-477.
[19] Zhang, B. Y., Li, H. H., & Wang, W. (2015). Numerical study of dynamic response and failure analysis of spherical storage tanks under external blast loading. *Journal of Loss Prevention in the Process Industries*, *34*, 209-217. https://doi.org/10.1016/j.jlp.2015.02.008
[20] Li, X., Chen, G., Khan, F., Lai, E., & Amyotte, P. (2022). Analysis of structural response of storage tanks subject to synergistic blast and fire loads. *Journal of Loss Prevention in the Process Industries*, *80*, 104891. https://doi.org/10.1016/j.jlp.2022.104891
[21] Sohaib, M., Islam, M., Kim, J., Jeon, D. C., & Kim, J. M. (2019). Leakage detection of a spherical water storage tank in a chemical industry using acoustic emissions. *Applied Sciences*, *9*(1), 196.
[22] Drosos, J. C., Tsinopoulos, S. V., & Karabalis, D. J. (2019). Seismic retrofit of spherical liquid storage tanks with energy dissipative devices. *Soil Dynamics and Earthquake Engineering*, *119*, 158-169. https://doi.org/10.1016/j.soildyn.2019.01. 003
[23] Qananah, R., Petrović, R. et al. (2022). Stress state optimisation of vertical atmospheric large-volume tanks. *Structural Integrity and Life*, *22*(2), 247-251.
[24] He, Z., Yuan, S., &Wang, Z.R. (2008). Deformation of revolving closed-shell with multi-curvature profile under inner pressure. *Journal of Materials Processing Technology*, *206*, 400-404.
[25] Kojić, M. (2002). An extension of 3-D procedure to large strain analysis of shells. *Computer Methods in Applied Mechanics and Engineering*, *191*, 2247-2462.
[26] Petrović, R., Živković, M., Topalović, M., & Slavković, R. (2015). Analytical, numerical and experimental stres sassessment of the spherical tank with large volume, *Tehnicki vjesnik*, *22*(5), 852-855. https://doi.org/10.17559/TV-20130905131504

Contact information:

Hana R. QANANAH
University "Union-Nikola Tesla",
Faculty of Information Technology and Engineering,
Belgrade, Serbia

Radovan PETROVIĆ, Professor
(Corresponding author)
University "Union-Nikola Tesla",
Faculty of Information Technology and Engineering,
Belgrade, Serbia
E- mail: radovan4700@yahoo.com

Maja ANDJELKOVIĆ, Professor
University "Union-Nikola Tesla",
Faculty of Information Technology and Engineering,
Belgrade, Serbia

Boris DAMJANOVIĆ
University "Union-Nikola Tesla",
Faculty of Information Technology and Engineering,
Belgrade, Serbia
E-mail: info@fiti.edu.rs

Igor MARTIĆ, D.Sc.
Innovation Center of Faculty of Mechanical Engineering,
Kraljice Marije 16, 11120 Belgrade, Serbia
E-mail: imartic@mas.bg.ac.rs

Ivana VUCETIĆ, D.Sc.
Innovation Center of Faculty of Mechanical Engineering,
Kraljice Marije 16, 11120 Belgrade, Serbia
E-mail: ivucetiic@mas.bg.ac.rs

Gordana DJUKANOVIC, Professor
Faculty of Forestry,
University of Belgrade, Serbia